# Deep learning for analysing synchrotron data streams

Boyu Wang[1], Ziqiao Guan[1], Shun Yao[1], Hong Qin[1], Minh Hoai Nguyen[1], Kevin Yager[2] and Dantong Yu[2]
Department of Computer Science
Department of Biochemistry and Structure Biology
Stony Brook University
Stony Brook, U.S.A.

The Center for Functional Nanomaterials
Computational Science Initiative
Brookhaven National Laborary, Upton, U.S.A.{boyu.wang, ziqiao.guan, shun.yao, qin, minhhoai}@stonybrook.edu,
{kyager,dtyu }@bnl.gov

***Abstract*—The National Synchrotron Light Source II (NSLS-II) at Brookhaven National Laboratory (BNL) is now providing some of the world's brightest x-ray beams. A suite of imaging and diffraction methods, exploiting megapixel detectors with kilohertz frame-rates at NSLS-II beamlines, generate a variety of image streams in unprecedented velocities and volumes. A complete understanding of a complex material system often requires a cluster of x-ray characterization tools that can reveal its elemental, structural, chemical and physical properties at different length-scales and time-scales. The flourish and continuing refinement of x-ray probes enable that the same sample may be studied with different perspectives and granularities, and at different time and locations; these powerful tools generate a correspondingly daunting big data challenge, with multiple image streams that outpaces any manual efforts and traditional data analysis practice. In this paper, we applied deep learning methods, in particular, deep convolutional neural network (CNN) to automatically recognize image features from image streams from NSLS-II, and integrated our deep-learning methods into the Google Tensorflow to cluster and label both real and synthetic 2-D scattering image patterns. These methods would empower scientists by providing timely insights, allowing them to steer experiments efficiently during their precious x-ray beamtime allocation. Experiment shows that the CNN-based image labeling attains a 10% improvement over traditional K-mean and Support Vector Machine.**

**Keywords—X Ray Image Classification, Deep learning, CNN**

## I. INTRODUCTION

X-ray scattering is a powerful technique for probing the physical structure of materials at the molecular and nanoscale, where strong x-ray beams are shined through a material to learn about its structure at the molecular level. This can be used in a wide variety of applications, from determining protein structure to observing structural changes in materials. Modern x-ray detector can generate 50,000 to 1,000,000 images/day (1-4 TB/day), thus it's crucial to automate the workflow as much as possible.

However, the current standard workflow in an x-ray scattering experiment consists of an experimental team traveling to a synchrotron beamline, capturing a detailed dataset over several days, and then returning to their home institution with the images for later analysis. The lack of immediate feedback during the experiment limits the scientific productivity. To reduce this data-analysis bottleneck, we explored the use of machine learning and computer vision to automate the process of image analysis.

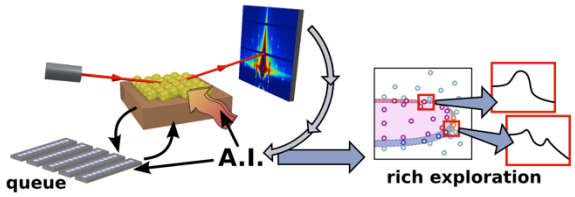


Fig. 1. Illustration of a computer-directed beamline experiment. The x-ray scattering experiment is controlled by A.I. software that runs a deep learning algorithm and has access to a stream of samples. The software automatically analyzes the stream of x-ray scattering images, clustering them and organizing them so as to generate scientifically-meaningful results. The extracted trends are used to inform further automated measurements, leading to a rich exploration of parameter spaces.

We envision a transformative paradigm for synchrotron studies, where data acquisition and analysis are automated, and scientists are thereby liberated to focus on deep scientific questions, rather than micro-managing the experiment. Towards this goal, we propose to develop a set of intelligent automated methods, which will be the "brain" of a computed-directed beamline experiment, as illustrated in Figure 1. These methods will be used in real-time to extract hierarchical and physically-meaningful insights from scientific datasets collected at NSLS-II beamlines: 1) Low-level: identifying characteristic features in a diffraction image; 2) Intermediate-level: detecting the occurrence of a physical process from a sequence of images; and 3) High-level: learning and predicting scientifically-meaningful trends.

Machine Learning itself is undergoing a shift, with a re-thinking from traditional, naive, neural networks, towards deep learning models where the neural hierarchy is more rational, optimized, and informative. This has already led to clear advances in several fields including computer vision and speech recognition, and we aim to demonstrate similarly transformative gains with respect to scientific image streams. The core idea in deep learning is to design multiple levels of representations corresponding to a hierarchy of features, wherein the high-level concepts and knowledge are derived from the lower layers. This multi-level representation can capture the complex relationships hidden within rich datasets.



978-1-4673-9051-4/16/$31.00 ©2016 IEEE

This hierarchical representation motif closely matches how scientific knowledge is organized, and indeed how physical systems can be understood, as illustrated in Figure 2.

To the best of our knowledge, only one paper addresses the classification of x-ray scattering images, examining 7 different features commonly used in computer vision [5]. However, most of image processing algorithms, such as HOG, LBP, and SIFT, are traditionally used with conventional images (e.g. photographs). In addition, many of the algorithms that are used in this context depended on image gradients of the boudaries of an object. Since x-ray scattering images lack discernable objects, edge detection is not as well-suited for this task, so the algorithms may not have performed as well as intended.

In this paper, we investigate deep learning based feature extraction for x-ray scattering images, and compare with traditional dictionary-based approaches.

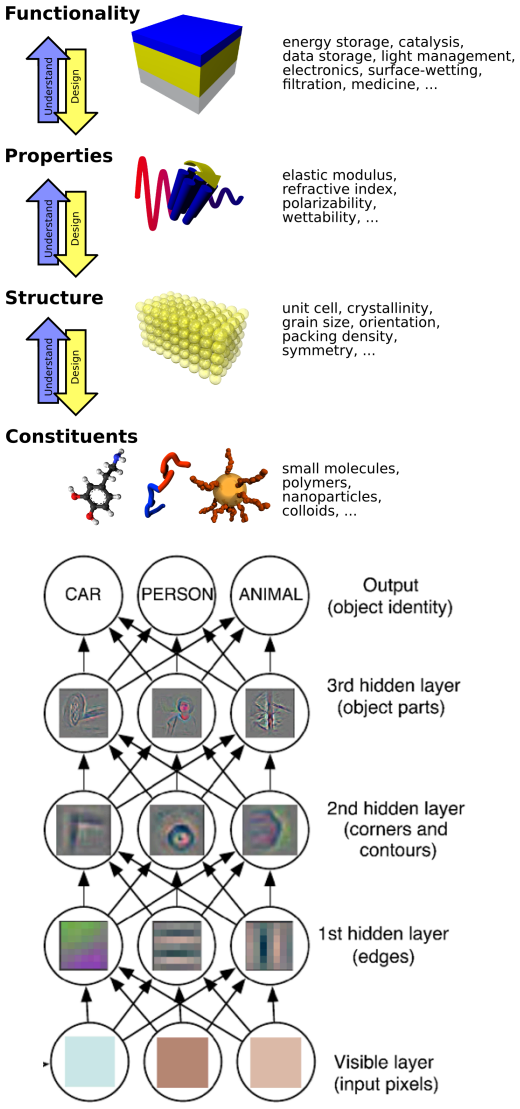


Fig. 2. Comparison of hierarchies underlying physical systems and deep learning models. Constituents organize into well-defined structures, which give rise to emergent properties, which in turn dictate functional response. By developing a machine-learning hierarchy closely aligned with this physically-relevant hierarchy, we will enable meaningful insights to be automatically extracted from scientific data at multiple levels. Similarly, deep learning recognizes raw images represented as a collection of pixel values to an object identify by breaking the complicated mapping into a series of simple mappings recursively, which creates a hierarchy. The input pixels are fed to the bottom visible layer, then a series of hidden layers abstract complex features from the lower layer. Both of them demonstrate similarity in feature extractions.

## II. Methods

### A. Dataset

We use two datasets. The first is a 'real' dataset of experimentally-measured x-ray scattering images [5], collected by casting a powerful x-ray beam through a collection of samples; in this dataset, each image was labeled by a materials scientist expert. The second dataset is a collection of synthetic scattering images, generated by simulation software. The simulation software generates artificial scattering images based on the known physics underlying x-ray scattering experiments, and adds add-hoc features meant to emulate the artifacts and defects that present in experimental images (e.g. shot noise).

In the experimental dataset, there are 2832 gray-scale x-ray scattering images in total, obtained during 13 different x-ray scattering measurement runs — a set of related x-ray scattering images collected for closely-related material samples, continuously captured over a short time period. All of the images have been labeled with 104 binary attributes by a domain expert. These attributes represent a diverse set of characteristics ranging from the type of measurement, to appearance based scattering features, to chemical composition and physical properties of the mate- rials. The list of all tags and its correponding number is in Figure 5.

We also visualized some of x-ray images as shown in Figure 3 and 4. In Figure 4, we show 2 different x-ray images collected in a different experimental geometry: small-angle x-ray scattering (SAXS) and wide-angle x-ray scattering (WAXS). In Figure 5, we show x-ray images exhibiting the same tag: 'ring'. Each image may include a diverse selection of image features, i.e., tags, which makes classification of x-ray scattering images difficult.

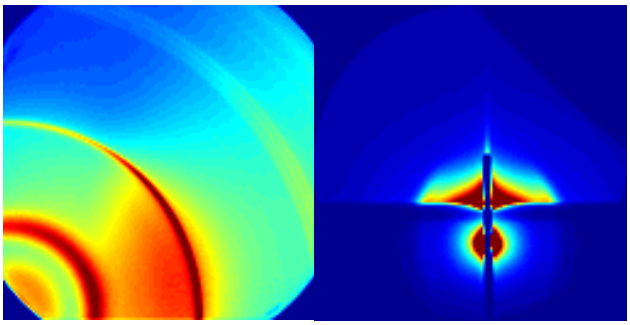

Fig. 3. Images in false color from real X-ray scattering dataset images The left image uses wide-angle x-ray scattering (WAXS), while the right image uses small-angle x-ray scattering (SAXS)

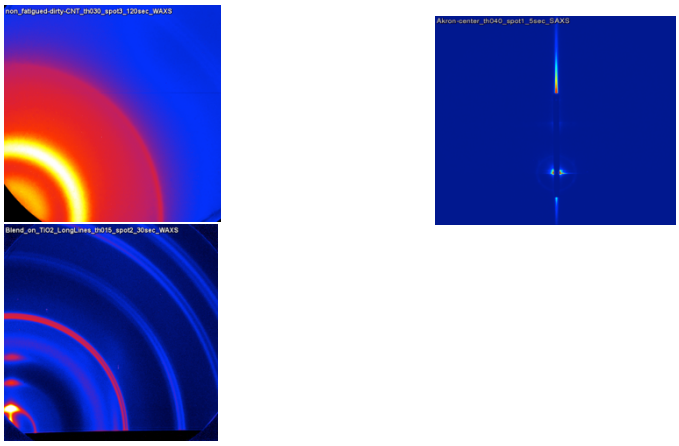

Fig. 4. Example of false color images with the "Ring" tag. Tags can include a diverse selection of images, which makes classification of x-ray scattering images difficult

| Attribute | # | Attribute | # |
|---|---|---|---|
| Thin film [G5] | 1646 | Silicon [G7] | 130 |
| Specular rod [G3] | 1597 | GTSAXS [G1] | 127 |
| Beam off image[G2] | 1591 | MWCNT [G7] | 125 |
| Photonics CCD[G2] | 1591 | Nanoporous [G5] | 125 |
| Ordered [G5] | 1462 | Theta sweep [G1] | 109 |
| GIWAXS [G1] | 1439 | PDMS [G7] | 107 |
| MarCCD [G2] | 1241 | Saturation artifacts [G3] | 97 |
| Horizon[G4] | 1171 | Peaks: Line z [G4] | 90 |
| Linear beamstop [G2] | 1156 | Circular beamstop [G2] | 85 |
| Peaks: Isolated[G4] | 1099 | Peaks: Line xy [G4] | 79 |
| GISAXS[G1] | 870 | Diffuse low-q: Anisotropic [G4] | 78 |
| Ring: Oriented z [G4] | 856 | Many rings [G4] | 78 |
| Polymer [G6] | 821 | Diffuse low-q: Oriented z [G4] | 76 |
| Halo: Isotropic [G4] | 791 | Misaligned [G3] | 76 |
| Ring: Isotropic [G4] | 604 | Beam streaking [G3] | 70 |
| Ring: Textured [G4] | 528 | Diffuse low-q: Oriented xy [G4] | 69 |
| Higher orders: 2 to 3 [G4] | 513 | Blocked [G3] | 62 |
| P3HT [G7] | 505 | Diffuse specular rod [G4] | 62 |
| Ring: Oriented xy [G4] | 491 | Smeared horizon [G4] | 55 |
| SiO2 [G7] | 467 | Symmetry ring: 4-fold [G4] | 55 |
| Vertical streaks [G4] | 434 | Higher orders: 10 to 20 [G4] | 53 |
| Single crystal [G5] | 430 | Ring doubling [G4] | 53 |
| Block-copolymer [G6] | 416 | Halo: Anisotropic [G4] | 46 |
| Peaks: Many/field [G4] | 396 | Powder [G5] | 44 |
| Grating [G5] | 375 | Specular rod peaks [G4] | 41 |
| PCBM [G7] | 369 | AgBH [G7] | 40 |
| Diffuse high-q: Isotropic [G4] | 357 | Ring: Oriented other [G4] | 33 |
| Higher orders: 4 to 6 [G4] | 351 | Peaks: Line [G4] | 23 |
| Weak scattering [G3] | 318 | Diffuse high-q: Oriented z [G4] | 20 |
| Rubrene [G7] | 266 | Bad beam shape [G3] | 19 |
| TSAXS [G1] | 264 | LaB6 [G7] | 16 |
| Higher orders: 7 to 10 [G4] | 260 | Phi sweep [G1] | 16 |
| 2D detector obstruction [G3] | 224 | Peak doubling [G4] | 15 |
| Bragg rods [G4] | 211 | Halo: Oriented xy [G4] | 14 |
| Ring: Anisotropic [G4] | 205 | Polycrystalline [G5] | 14 |
| Peaks: Along ring [G4] | 201 | Diffuse high-q: Oriented xy [G4] | 11 |
| Amorphous [G5] | 197 | Direct [G3] | 11 |
| Saturation [G2] | 193 | Object obstruction [G3] | 9 |
| PS-PMMA [G7] | 190 | Peaks: Line other [G4] | 9 |
| Composite [G5] | 179 | Waveguide streaks [G4] | 8 |
| Diffuse low-q: Isotropic [G4] | 170 | Higher orders: 20 or more [G4] | 4 |
| Yoneda [G4] | 167 | Substrate streaks/Kikuchi [G4] | 4 |
| Strong scattering [G3] | 159 | Diffuse low-q: Oriented other [G4] | 3 |
| TWAXS [G1] | 152 | Halo: Spotted [G4] | 3 |
| Halo: Oriented z [G4] | 148 | Diffuse low-q: Spotted [G4] | 2 |
| High background [G4] | 142 | Diffuse high-q: Spotted [G4] | 1 |
| Asymmetric (left/right) [G2] | 138 | Empty cell [G3] | 1 |
| Ring: Spotted [G4] | 136 | Parasitic slit scattering [G3] | 1 |
| Superlattice [G6] | 136 | Point detector obstruction [G3] | 1 |

Fig. 5. List of the 104 tags used in this experiment and their counts and staticstics.

### *B. Traditional Methods*

In this section, we explore tradictional Bag-of-Features (BoF) and Spatial Pymaid Matching (SPM) [6,7,8] based approach for X-ray image classification. Bag-of-Features is a widely used approach for feature extraction. In each image, we random sample 1000 image patches (including multiple scales). Then a dictionary of patches are built using k-means clustering algorithm. After forming the k-means dictionary, every patch in each image is assigned to a cluster.

Next, we perform three-level spatial pyramid matching. At each level, we subdivide the image into "bins" and compute the histograms at each bin, weighing each histogram a certain amount. This approach allows the classifier to better understand the spatial relationship between different areas of an image. In this experiment, we used sum pooling, since we are computing histograms and we need the frequency of each cluster.

After extracting features, an SVM [9] with exponential chi-square kernels is used for the classification.

### *C. Deep learning based approach*

Deep learning has achieved huge success for image classication in recent years. The breakthough in the area is mainly because of huge amount of data available and good network architecture. Alex-Net is the first Convolutional Neural Network that has successfully applied in this area.

Instead of using hand-crafted image features for image classification, neural network can be used to learn features for image classification. However, it requires many customization and hand tunings to attain an effective and efficient implementation. The basic units in Convolutional Neural Network (CNN) are:

- Convolutional Layer: A fully connected network requires an excessive number of free parameters. Instead, we apply a convolutional neural network (CNN) that allows sharing parameters among different image patches. As a result, CNN reduces the number of parameters, and automatically discovers local patterns. Figure 6 shows the comparison between fully connected neural network and convolution neural network.
- Subsampling / Pooling Layer: Pooling Layer allows local patterns to be pooled in a large region as Figure 7 shows [10].
- Activation Layer: Non-linear Activation allows the neural network to learn non-linear functions. Traditional activation layers utilize sigmoid fuction. However, the problem of sigmoid is that the gradient decreases significantly during the back-propogation processing across many layers of deep networks. In addition, sigmoid is easy to saturate, when it's saturated, the gradient is close to 0. If the network has multiple sigmoid layers, the gradient at early layer will be every small, which make the parameters of early layers hard to optimize. Instead, the most widely used activation function is Rectified-Linear Units (ReLU). If the

value is below 0, the output of ReLU is 0, otherwise, the output is the same as input. Figure 8 show shows the comparision of sigmoid and ReLU [10].

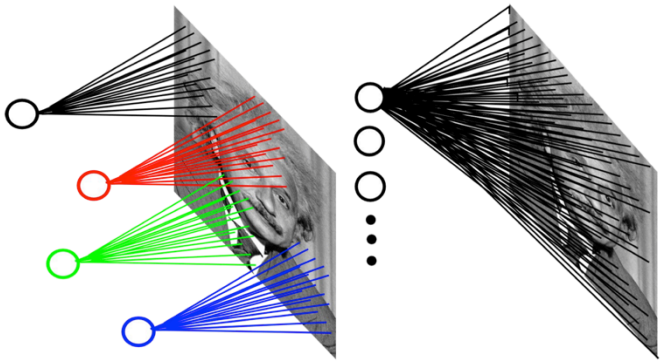

Fig. 6. Comparison between fully connected neural network (left) and convolutional neural netowrk (right). With parameter sharing, CNN is able to reduce the number of parameters.

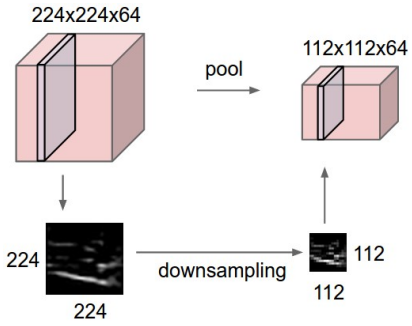


Fig. 7. Subsampling / Pooling Layer

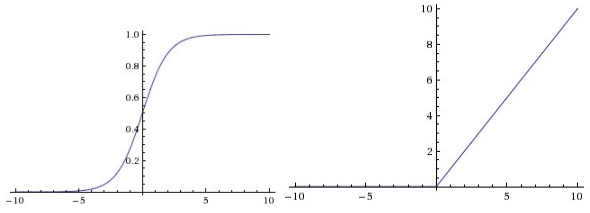

Fig. 8. Comparison between different activation function: sigmoid (left) and ReLU (right)

We use the stochastic gradient descent based approach (SGD) to train CNN. The entire dataset is divided into multiple batches. Each batch contains ten to one hundred images. The gradient with respect to parameters is computed in each batch to estimate the gradient across whole dataset.

In this experiment, we adopt Alex-Net based architecture for x-ray scattering image classification, but with following changes: We changed the last layer from softmax layer to sigmoid layer, where the output has dimension the same as the number of tags. Each output represents the probability of having that specific attribute.

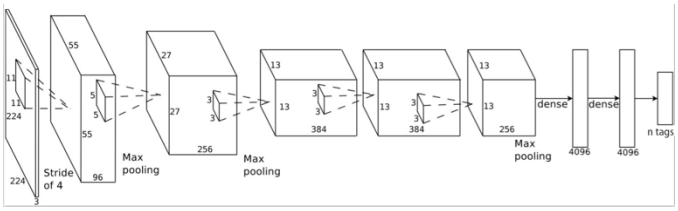


Fig. 9. CNN Network architecture overview. We use Alex-Net based architecture, which contains 5 layer convolutional layers. We changed the last layer from softmax layer to sigmoid layer, since one image could have multiple tags

## III. EXPERIMENTS

### A. *Traditional Methods*

We perform BoF and SPM based approach on both experimental x-ray images and synthetic x-ray images. The number of clustering we choose is 2000. There are 104 possible tags for the images. However, some tags had very few images associated with them, so we eliminated 12 tags with less than ten images. In addition, we considered six high-level attributes found in [5], bringing the number of tags used to 98. We use average precision (AP) for performance evaluation.

For synthetic dataset is much unbalanced compared the real dataset, so we group further grouped the number of tags into 20 high level attributes for evaluation.

TABLE I. TRADITIONAL METHODS RESULTS

| | ***Real Dataset*** | ***Synthetic Dataset*** |
|---|---|---|
| Mean Average Precision | 0.6018 | 0.6705 |

### B. *Deep learning based approach*

Since we only have 2832 experimental x-ray Scattering image, it is hard to train a CNN based on those images. Thus, we generate 100,000 synthetic x-ray images to train CNN. The network we are using is based on Alex-Net. The number of parameters in our network is about 72 million. Due to the large unbalanced problem of the data (as Figure 5 shows, some tags are really rare), we take a sublist of 17 most frequent tags and the CNN is trained on those tags. Figure 10 shows the training loss across different epochs (every epoch goes through the whole dataset).

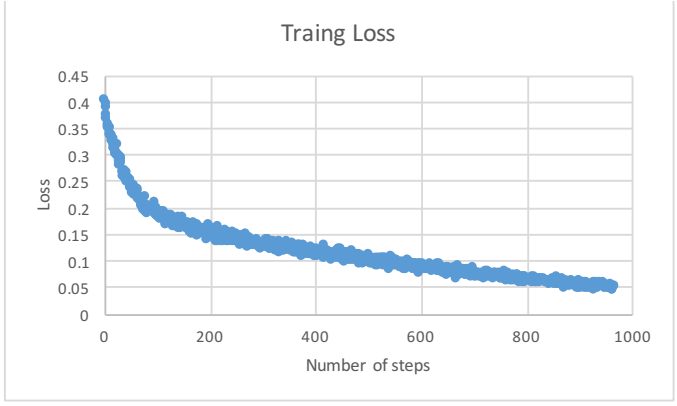


Fig. 10. Training Loss

We also report the mean Average Precision using Deep learning in Table 2. From the results, we notice that the CNN based approach outperforms BoF and SPM based approach by a large margin.

TABLE II. CNN BASED RESULTS

| | ***Synthetic Dataset*** |
|---|---|
| Mean Average Precision | 0.771 |

## IV. CONCLUSION

In this work, we addressed the complexity of hierarchical self-assembling nano-materials by developing a corresponding hierarchy of deep learning methods. We integrated our deep-learning methods into the Google Tensorflow software to cluster and label both real and synthetic 2D scattering image patterns. The preliminary results from our intensive cross-validation processing showed that deep learning networks, with a minimal tuning, easily attained better performance compared to traditional methods.

## V. FUTURE WORK

With the help of simulation software, we may generate more images that have rare tags to train the Convolution Neural Network and hope to mitigate the unbalanced dataset problem. We will also test our network trained on synthetic dataset on real X-ray images to automate the current workflow as much as possible.

## REFERENCES


[1] Brody Huval, Tao Wang, Sameep Tandon, Jeff Kiske, Will Song, Joel Pazhayampallil, Mykhaylo Andriluka, Pranav Rajpurkar, Toki Migimatsu, Royce Cheng-Yue, Fernando Mujica, Adam Coates, and Andrew Y. Ng. An empirical evaluation of deep learning on highway driving. *CoRR*, abs/1504.01716, 2015. URL http://arxiv. org/abs/1504.01716.

[2] Alex Krizhevsky, Ilya Sutskever, and Geoffrey E. Hinton. Imagenet classification with deep convolutional neural networks. In F. Pereira, C. J. C. Burges, L. Bottou, and K. Q. Weinberger, editors, *Advances in Neural Information Processing Systems 25*, pages 1097–1105. Curran Associates, Inc., 2012. URL http://papers.nips.cc/ paper/4824-imagenet-classification-with-deep-convolutional-neural-networks. pdf.

[3] Yann LeCun, Yoshua Bengio, and Geoffrey Hinton. Deep learning. *Nature*, 521(7553):436–444, 2015.

[4] Salah Rifai, Yann N Dauphin, Pascal Vincent, Yoshua Bengio, and Xavier Muller. The manifold tangent classifier. In *Advances in Neural Information Processing Systems*, pages 2294–2302, 2011.

[5] Kiapour, M. Hadi, et al. "Materials discovery: Fine-grained classification of X-ray scattering images." *IEEE Winter Conference on Applications of Computer Vision*. IEEE, 2014.

[6] S. Lazebnik, C. Schmid and J. Ponce, 'Beyond Bags of Features: Spatial Pyramid Matching for Recognizing Natural Scene Categories', *2006 IEEE Computer Society Conference on Computer Vision and Pattern Recognition - Volume 2 (CVPR'06)*, 2006.

[7] T. Serre, L. Wolf and T. Poggio, 'Object Recognition with Features Inspired by Visual Cortex', *2005 IEEE Computer Society Conference on Computer Vision and Pattern Recognition (CVPR'05)*, 2005.

[8] J. Yang, K. Yu, Y. Gong and T. Huang, 'Linear spatial pyramid matching using sparse coding for image classification', *2009 IEEE Conference on Computer Vision and Pattern Recognition*, 2009.

[9] Chih-Chung Chang and Chih-Jen Lin, LIBSVM : a library for support vector machines. ACM Transactions on Intelligent Systems and Technology, 2:27:1--27:27, 2011. Software available at http://www.csie.ntu.edu.tw/~cjlin/libsvm

[10] Convolutional Neural Network for Visual Recognition URL http://cs231n.github.io/convolutional-networks/